

## Chapter 3

# IRF applied to the transit of CoRoT planets

In this chapter, the IRF is applied to the CoRoT light curves of the first seven planets and brown dwarf discovered by CoRoT. The phase folded transits of the IRF-filtered light curves are fitted to derive the planet parameters using a Levenberg-Marquardt algorithm and the analytical transit models of Mandel & Agol (2002). The results are compared to the parameters published in the planet/brown dwarf discovery papers.

Some of the work presented in this chapter has been published: in Fridlund et al. (2010) for the work on CoRoT-6b and in Léger et al. (2009) for the work on CoRoT-7b. The IRF was used as an independent analysis of the transit light curves. The method was optimised further since these publications, especially in the understanding (strengths and limitations) of the IRF and of the techniques used to find the best model to the transit.

### 3.1 Description of the CoRoT data

#### 3.1.1 Instrument

CoRoT (Convection, Rotation and planetary Transits)<sup>1</sup> is a modest scale mission (626 kg satellite, 80 million euros in cost) primarily funded by the French space agency CNES (Centre National d'Etude Spaciale), with contributions from ESA (European Space Agency), Belgium, Austria, Germany, Spain and Brazil. The satellite was launched on December 27th 2006 into a polar orbit at  $\sim 900$  km of altitude.

CoRoT is the first space-based telescope designed for high precision photometry with long time coverage after MOST<sup>2</sup> (150 days for the long runs and 20-30 days for the short runs, with duty cycle greater than 93%). Aigrain et al. (2009) evaluated the noise

---

<sup>1</sup>Official CoRoT website: <http://corot.oamp.fr>

<sup>2</sup>The MOST (Microvariability and Oscillations of STars telescope) satellite, launched in 2003, has a diameter of 15cm and stares at each single field for about 30 days.

level of real CoRoT data on 2h timescale at 0.1 mmag and 1 mmag for R magnitude of 11.5 and 16 respectively. CoRoT is designed to perform two types of science: stellar seismology (to study stellar interiors), and exoplanet transits search. In this thesis, we are interested in the planet-finding channel of CoRoT. Over the nominal duration of the mission, in the exoplanet channel, CoRoT will have observed over 12000 stars ( $V > 16.5$ ) per run. CoRoT nominal duration is three years, and has been extended for another three years. CoRoT operates at half field of view since March 2009, due to a problem effecting two of its four CCDs.

The telescope is afocal and has a 27 cm diameter primary mirror and a baffle (to prevent reflected light from the Earth reaching the CCDs). CoRoT has two 6-month viewing zones each year, pointing from April to October towards the galactic anti-centre ( $RA \sim 6^h50^m$ ,  $DEC \sim 0^\circ$ ) in the constellations of Aquila and Serpens Caput, and from October to April towards the Galactic centre ( $RA \sim 18^h50^m$ ,  $DEC \sim 0^\circ$ ) in the constellation of Monoceros.

In the exoplanet channel, there are two 2048 x 2048 pixels CCDs with a combined field of view of  $1.3^\circ \times 2.6^\circ$ . A bi-prism, placed in the optical path, disperses the light and provides a very low-resolution spectrum of each star (light divided into blue, green and red channels). This is intended to help identify transit like events caused by stellar binary systems or stellar activity, as stellar dependent effects are chromatic while planetary transits are not.

A general description of the CoRoT science objectives can be found in Baglin et al. (2006), and a technical description of CoRoT in Boisnard & Auvergne (2006) and in the CoRoT instrument handbook<sup>3</sup>. Auvergne et al. (2009) describe the CoRoT satellite in flight performance.

### 3.1.2 Light curve generation

The different levels of light curve generation are summarised in Baudin et al. (2006).

#### Treatment on board

Due to a limited telemetry rate (1.5 Gbit per day), aperture photometry is performed and co-added on board the satellite and then downloaded to Earth. The raw data (time stamped aperture photometry of each star) received on Earth are labelled N0 data.

As the image of each star (PSF, point spread function) is tear-shaped due to the diffraction through the bi-prism, the aperture photometry is done with a tear-shaped mask – chosen among 256 templates depending on the star magnitude, temperature and position on the CCD but fixed for each star during a given run. A mask has typically between 50 and 100 pixels. For most of the stars, all the light falling inside the mask

<sup>3</sup>CoRoT instrument handbook: <http://corotsol.obspm.fr/web-instrum/payload.param/>

(white light, 300 to 1000 nm) is integrated on board and downloaded to Earth. For a selection of up to 5000 stars with  $R$  magnitude less than 15, the mask is divided into three bands (blue, green and red channels), the light is integrated within each band and three colour stellar flux is computed on board and downloaded to Earth.

The integration time of each exposure is 32 s. The aperture photometry is co-added on board every 512 s. For 500 selected stars showing sharp flux variations (potential transit candidates), the 32 s rate is downloaded to Earth.

### Treatment on the ground

On the ground, the N0 photometry is pipeline-processed to correct (and/or flag) anticipated astrophysical and instrumental noise effects (e.g. background, high energy particles during the crossing of the South Atlantic Anomaly, satellite jitter, outliers e.g. images of debris or high energy particles). The pipeline also transform the CoRoT time stamps into HJD (Heliocentric Julian Date), and the electron counts into stellar flux. The flux-time series (the light curves) are then produced for each star, these data are labelled N1.

Information from preliminary observations (e.g. stellar magnitude) are added as keywords in the header of the N1 data. The resulting files are labelled N2. The N2 data are ready for scientific analysis and released to the CoRoT Co-Investigators a few months after the end of each run and to the public<sup>4</sup> a year later.

The steps of the N1 to N2 data was also intended to correct for common noise sources identified in all the N1 light curves (e.g. using *SysRem* described in Tamuz et al. 2005 and Mazeh et al. 2009), but this is in practice implemented on the N2 data by the CoRoT scientific team on a case to case basis.

With practice on the real CoRoT data, additional noise effects affecting all the light curves have been identified, such as:

- the temperature variation of the satellite when it passes through the Earth's shadow cone causing satellite pointing jitters and stellar flux drops as some flux falls outside the aperture mask. This effect can be corrected as it is a systematic effect affecting simultaneously all the stars and hence their light curve, with a method such as was described in Mazeh et al. (2009). Points in the light curve affected by this effect are flagged in the new N2 data (N2v2). The data used in this chapter are from the previous N2 data.
- hot pixels which are due to high energy particle hits on some pixels. These hits affect the electronic response of the pixels which translates into sharp flux jumps and flux decay in the light curve. This effect is more difficult to systematically correct from. Drummond et al. (2008) discuss methods to tackle this issue but none so far can be used in a fully automated way.

<sup>4</sup>CoRoT data archive: <http://idoc-corot.ias.u-psud.fr>

When solutions to correct these noise effects are known and well tested, corrections to these effects are included to the pipeline producing the N2 level light curves. The photometry used in this chapter was performed using the latest version of the CoRoT reduction pipeline. This new version of the pipeline uses the information about the instrument's PSF and the centroids of the stars measured in the asteroseismology channel to correct the effects of the satellite jitter in the white light curve.

### 3.1.3 Additional light curve pre-processing

The light curves used in this chapter are the N2 data. In these light curves, several common effects are present:

- upward outliers due to high energy particle hits (such as during the South Atlantic Anomaly crossing) causing an increase in the background level
- downward outliers due to the satellite entry and exit from the Earth's shadow causing a temporary loss of pointing accuracy resulting in a drop in flux
- long term downward trend due to instrumental performance decay or pointing drift
- variations on timescales of days to weeks caused by rotational modulation of active regions on the stellar surface
- sudden discontinuities called "hot pixels" caused by high energy particles hits on one or more pixels temporally affecting the sensitivity of these pixels. The decay of the pixel back to its original non-excited level can be smooth or sudden

The approach adopted here to correct for these effects is the following. The upward and downward outliers are identified by an iterative non-linear filter (Aigrain & Irwin, 2004), also described in Chap 2 Section 2.3.1) consisting of 5 iterations with a 5-points boxcar filter, a 1-hour median filter and a  $3\sigma$  outliers identification. The downward outliers are flagged by the N2 pipeline. The flagged outliers are removed from the light curve.

The long term downward trend, the smooth decay after "hot pixels" and the stellar flux modulation are modelled and corrected using the iterative reconstruction filter (IRF, Alapini & Aigrain 2009, also described in Chap 2, Section 2.4.1), with the filtering timescales adapted to each stellar variability signal and transit signal. The IRF has the advantage of using only two free parameters which are the smoothing lengths used to estimate the signal at the planet's orbital period and the signals at other timescales – including the stellar variability. The former represents a compromise between reducing the noise and blurring out potential sharp features associated with the planet, and the latter between removing the stellar signal and affecting the planetary signal.

The iterative reconstruction filter works on uniformly sampled light curves so any part of

each light curve sampled at 32 s is resampled to 512 s before running this filter. The iterative reconstruction filter cannot thoroughly remove very sharp flux variations such as those caused by "hot pixels" (the residuals of these hot pixels are visible at a  $10^{-3}$  level in the phase-folded light curve), so the regions of light curve affected by sharp flux variations are clipped out before running the IRF.

### 3.1.4 Planetary transit detection and confirmation

The light curves from each run are systematically searched for planetary transits and priority-ranked by several teams (France: LAM, IAS, LESIA, LUTH; UK: Exeter; Germany: DLR, Köln; Spain: IAC; ESA: ESTEC; Austria: Graz). Each detection team uses its own set of pre-processing, de-trending and transit search tools (Moutou et al. 2005 describes most of them). Each team ranks the detected planetary-transit-like events with the same criteria: transit depth (planet-candidate to star radii ratio), signs of binary nature (secondary eclipses, ellipsoidal variations, transit depth different in the three colours), transit shape ("U" for central transits, "V" for grazing transits). The rankings are automatically merged to extract a list of high quality candidates for follow-up.

The follow-up consists of: ground-based in and out of transit photometry at high spatial resolution to spatially resolve the stars falling in the CoRoT aperture mask and identify which star is being eclipsed, multiple radial velocity measurements to derive the planet-candidate to star mass ratio, and a high resolution, high signal to noise spectrum of the host star to derive precise stellar parameters and hence precise planet parameters.

The parameters measured for each CoRoT planet are the orbital period  $P$ , the epoch of the centre of the first transit observed  $T_0$ , the planet orbital to plane-of-view inclination  $i$ , the orbital distance to stellar radius ratio  $a/R_*$ , and the planet to star radii ratio  $R_p/R_*$ . Some stellar parameters can also be derived from the light curve: the stellar mass to radius ratio  $M_*^{1/3}/R_*$  (derived directly from  $a/R_*$  and  $P$ ), the star rotation period  $P_{\text{rot}}$ , and the stellar limb darkening coefficient  $u_a$  (linear law) and  $u_b$  (second coefficient in quadratic law).

## 3.2 Primary transit parameters with the IRF-filtering

The work in this section was performed on the CoRoT space-photometry of the stars harbouring the first six planets and the first brown dwarf discovered by the CoRoT mission.

### 3.2.1 Method

We filter the light curve with the IRF (definition in Chap. 2, Sec. 2.4.1) to remove the flux variation intrinsic to the star. By default, the IRF is run with a bin size of 0.0006 in

phase (IRF `binsize` parameter, which controls the smoothing length used to estimate the phase-folded transit signal), and with a convergence limit of  $1 \cdot 10^{-8}$ . The `cvlim` parameter sets the convergence criterion. At each iteration, the residuals of the light curve with the last estimate of the stellar variability and the transit signals removed are compared with those of the previous iteration. `cvlim` is the maximum difference allowed between these two sets of residuals. To explore the performance of the IRF in evaluating the stellar variability signal with a given time scale (IRF `timescale` parameter, which controls the smoothing length used to estimate the stellar variability), two values of this parameters are tested systematically: 0.50 and 0.25. `timescale=0.10` days is also tested to see how the IRF behaves in the case of extreme filtering.

CoRoT has a large PSF due to the defocussing of the telescope and the prism in the optical path. It used different aperture masks (50 to 100 pixels each) to extract the photometric time series of the stars. Often in CoRoT photometry, a second star falls into the mask of the target star, contaminating the light of the latter. This is the case for the CoRoT light curves of the host stars of CoRoT-2b, CoRoT-3b, CoRoT-4b, CoRoT-5b and CoRoT-6b, with the following respective fractions of contaminant flux:  $5.6 \pm 0.3$  % (Alonso et al., 2008),  $8.2 \pm 0.7$  % (Deleuil et al., 2008),  $0.3 \pm 0.1$  % (Aigrain et al., 2008), 8.4% (Rauer et al., 2009), and  $2.8 \pm 0.7$  % (Fridlund et al., 2010). The transit of a planet in a light curve contaminated by the flux of another star, appears shallower. Thus, the flux from the contaminant star should be removed before deriving the planet parameters from the transit light curve. In this chapter, this is done by subtracting the fraction of the contaminant (e.g. -0.056 for 5.6%, the uncertainty on this flux is taken into account in the error estimate of the best transit model) from the normalised IRF-filtered light curve, and re-normalising the resulting light curve.

When an out-of-transit variation around the phase-folded IRF-filtered transit signal is observed, a  $2^{nd}$  order polynomial ( $y = a + b x + c x^2$ ) is fitted about the phase-folded IRF-filtered transit and divided into the transit. The phase range each side of the transit used to evaluate the polynomial fit is (0.015,0.025) for orbital period  $P > 10$  d, (0.04,0.08) for  $4 < P < 10$  d, and (0.1,0.2) for orbital period  $P < 4$  d.

The transit signal (corrected from the polynomial slope about the phase-folded transit when necessary) is then fitted using the analytical formulation of Mandel & Agol (2002). The method used to find the best fit to the transit light curve is non-linear least squares method, the Levenberg-Marquardt algorithm.

### Best fit with the Levenberg-Marquardt algorithm

The Levenberg-Marquardt algorithm is a method to efficiently find a local minimum in a nonlinear  $\chi^2$  space, given a good first estimate.

This thesis makes use of an IDL implementation of the Levenberg-Marquardt algorithm called MPFIT<sup>5</sup> and written by Craig Markwardt (Markwardt, 2009). MPFIT takes as in-

<sup>5</sup><http://www.physics.wisc.edu/~craigm/idl/fitting.html>

put a model function and the list of parameter values to be tried, evaluates the model for each of these parameters, returns the residuals of the data, and moves in the parameter space to find the minimum in  $\chi^2$  using a combination of Newton's method (adjusting search direction according to the curvature, i.e. the second derivative) and steepest-descent method (adjusting the steps according to the value of the gradient, i.e. the first derivative).

The limitation of the Levenberg-Marquardt method is that if the  $\chi^2$  space has several local minima and the initial guess are not close the true minimum, the algorithm might find a local minimum in the  $\chi^2$  space and not the true minimum. This is a problem when dealing with a complex  $\chi^2$  space, in which case using a Markov Chain Monte Carlo (Section 6.1) to find the true minimum is a more robust approach.

The adjusted parameters are the epoch of the first transit in the CoRoT light curve  $T_0$ , the system scale  $a/R_*$ , the inclination between the planet orbital plane and the plane-of-view  $i$ , and the planet-to-star radii ratio  $R_p/R_*$ . Also simultaneously adjusted are  $u_+$  and  $u_-$ , combinations of limb darkening coefficients ( $u_+ = u_a + u_b$  and  $u_- = u_a - u_b$  where  $u_a$  and  $u_b$  are the quadratic limb darkening coefficients). The choice of the quadratic law was made as it follows the limb darkening of a star better than a linear law, without adding too many additional free parameters. The eccentricity and angle to periastron are fixed to 0. The transit period is fixed to the value in the discovery paper of the planet, or to a refined value when needed. If a refined value of the period is needed, it is determined using Aigrain & Irwin (2004) transit search algorithm with a small period search window around the value in the planet discovery paper.

### Uncertainties on the parameters

Estimating the uncertainties on the derived parameters can be done in several ways:

- Alonso et al. (2008) evaluate the uncertainty on the planet parameters of CoRoT-1b using a bootstrap analysis. They randomly shuffle a fraction of the residuals, re-add the transit model and re-evaluate the planet parameters. They do this several thousand times and estimate the uncertainty on each planet parameter as the standard deviation of the values taken by this parameter. This method accounts for the white noise in the data.
- Aigrain et al. (2008) evaluate the uncertainties on the planet parameters of CoRoT-4b using a correlated bootstrap approach. They randomly shuffle intervals of the residuals of a chosen length (e.g. 1.12h avoiding aliases with periodic signals such as the satellite and Earth orbits), re-add the transit model and re-evaluate the planet parameters. They do this several hundred times and estimate the uncertainty on each planet parameter as the standard deviation of the values taken by this parameter. The fact that each interval is shuffled in its entirety preserves

the correlated noise on hourly timescales. This method thus accounts for both the white noise and the correlated noise in the data.

- Rauer et al. (2009) derive the planet parameters of CoRoT-5b using a Markov Chain Monte Carlo (MCMC) procedure. The uncertainty on a parameter is taken as the standard deviation of its posterior distribution. The uncertainties take into account the shape of parameter space around the best model.

Out of these three methods to derive the uncertainties, the later is the most robust. This approach is studied in Chapter 6. In the current chapter, the method adopted is similar to the second one. The uncertainties on the parameters of the best transit fit are evaluated by removing this fit from the IRF-filtered light curve, circularly permuting the residuals, re-inserting the best transit fit, re-fitting the resulting transit signal, doing the above 100 times, and evaluating the standard deviation of the parameters of the best fit for each parameter. Circularly permuting the residuals conserve the correlated features in the data and take them and the white noise into account when evaluating the uncertainties.

When the light curve was corrected from the light of a contaminant star, the uncertainty on the contaminant flux should be taken into account in the derivation of the uncertainties associated to the planet parameter. This is done by adding to each realisation of the noise (as described above) a constant drawn from a Gaussian distribution with zero mean and standard deviation equal to the uncertainty on the contaminant flux and re-normalising the resulting light curve. The uncertainties on the planet parameters are then derived from the different realisations as described previously.



### 3.2.2 CoRoT-1b

CoRoT-1b is a Jupiter-like planet orbiting its solar type host star in 1.5 days. This planet was observed with CoRoT for 55 days from February 6th 2007. The light curve was sampled every 512 s for the first 28 days, and then every 32 s for the remaining 24.7 d. The discovery of this planet was published in Barge et al. (2008). Radial velocity measurements were performed with SOPHIE<sup>6</sup> to confirm the planetary nature of the transiting companion. Further radial velocity measurements of the planet were performed with HARPS<sup>7</sup> to derive a precise mass for the planet. Table 3.1 lists the parameters derived for CoRoT-1b and its host star.

The period was refined using Aigrain & Irwin (2004) transit search algorithm. The new best period found is 1.5091897 days, this is the value that was used below for the IRF and the transit fits. The IRF cannot correct sharp flux variations, so before running the IRF, the points before HDJ-2451545=2594 and after HDJ-2451545=2638 were cut out. The IRF was run with the default values and the IRF-filtered transit signals were fitted, as described in Section 3.2.1. The resulting IRF-filtered light curves along with their transit fit are shown in Fig. 3.2, and the planet parameters in Table 3.1.

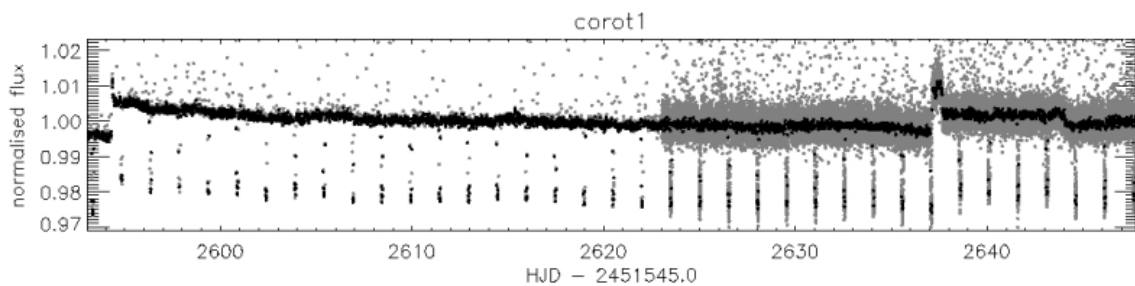


Figure 3.1: CoRoT-1's light curve (grey), re-binned with outliers clipped out (black).

<sup>6</sup>SOPHIE: 40000-resolution echelle spectrograph on the 1.93m telescope at the Observatoire de Haute Provence, France

<sup>7</sup>HARPS: 100000-resolution echelle spectrograph on the 3.6m telescope at ESO La Silla Observatory, Chile

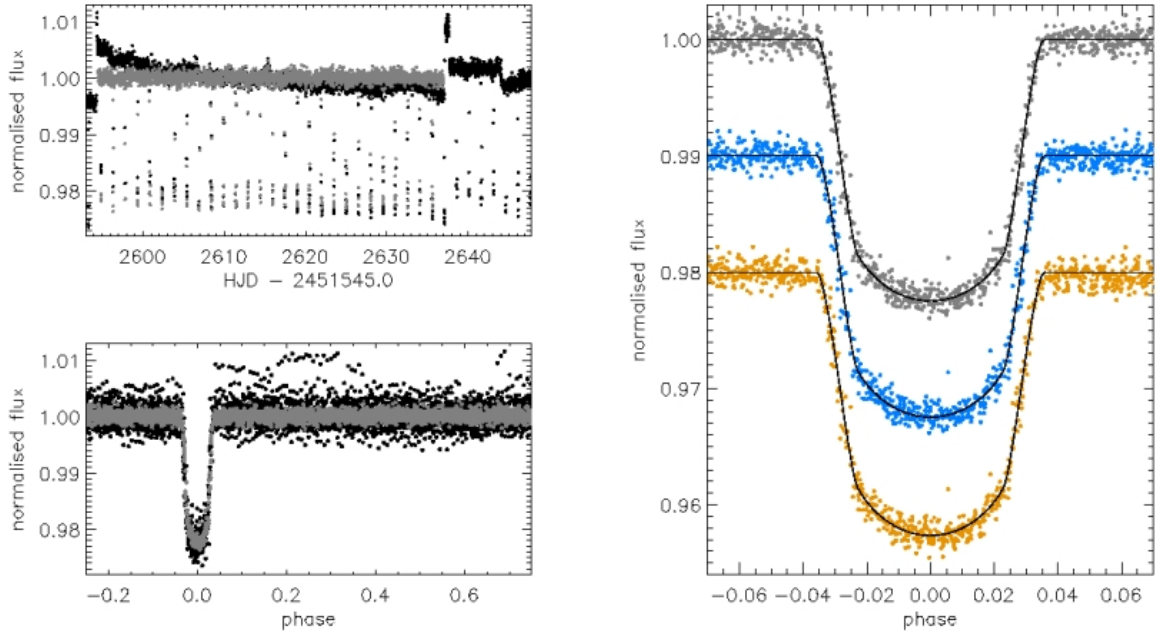


Figure 3.2: The IRF-filtered transit light curve of CoRoT-1b. Left panel: the IRF-filtered transit light curve with timescale=0.5 d (grey) superimposed on the pre-processed light curve (black), unfolded (top panel) and phase-folded (bottom panel). Right panel: the IRF-filtered light curve with timescale=0.5 d (grey), 0.25 d (blue) and 0.10 d (orange). The black lines are the best fits to each IRF-filtered transit, the planet parameters derived from these fits are shown in Table 3.1.

Table 3.1: Host star and planet parameters of CoRoT-1b.

Star	Barge et al. (2008)	this study		
		IRF 0.5d	IRF 0.25d	IRF 0.1d
RA (J2000)	06 <sup>h</sup> 48 <sup>m</sup> 19.17 <sup>s</sup>			
Dec (J2000)	-03° 06' 07.78''			
$V_{\text{mag}}$	13.6			
$v \sin i$ (km s <sup>-1</sup> )	5.2 ± 1.0			
$T_{\text{eff}}$ (K)	5950 ± 150			
log $g$	4.25 ± 0.30			
[Fe/H]	-0.3 ± 0.25			
$M_{\star}$ ( $M_{\odot}$ )	0.95 ± 0.15			
$R_{\star}$ ( $R_{\odot}$ )	1.11 ± 0.05			
<b>From light curve</b>				
$P$ (d)	1.5089557 ± 0.0000064	1.5091897 (fixed)	1.5091897 (fixed)	1.5091897 (fixed)
$T_0 - 2454159$ (d)	0.4532 ± 0.0001	0.45265 ± 0.00007	0.45265 ± 0.00007	0.45269 ± 0.00008
$R_p/R_{\star}$	0.1388 ± 0.0021	0.1433 ± 0.0005	0.1432 ± 0.0006	0.1437 ± 0.0008
$a/R_{\star}$	4.92 ± 0.08	4.56 ± 0.04	4.57 ± 0.04	4.54 ± 0.05
$i$ (°)	85.1 ± 0.5	83.1 ± 0.3	83.1 ± 0.3	83.0 ± 0.3
$u_a$	0.42 ± 0.34	0.49 ± 0.02	0.49 ± 0.02	0.51 ± 0.02
$u_b$	0.29 ± 0.34	0	0	0
$e$	0 (fixed)	same (fixed)	same (fixed)	same (fixed)
$\frac{M_{\star}^{1/3}}{R_{\star}} (M_{\odot}, R_{\odot})$	0.887 ± 0.014			
$b$	0.42 ± 0.05	0.55 ± 0.03	0.55 ± 0.03	0.55 ± 0.03
<b>Planet</b>				
$M_p (M_{\text{Jup}})$	1.03 ± 0.12			
$R_p (R_{\text{Jup}})$	1.49 ± 0.08			

### 3.2.3 CoRoT-2b

CoRoT-2 is an active solar-type star, its light curve is shown in Figure 3.3. CoRoT-2b is a Jupiter-like planet orbiting its host star in 1.7 days. This planet was observed with CoRoT nearly continuously for 152 days from May 16th 2007. The discovery of this planet was published in Alonso et al. (2008). Radial velocity measurements of the star were performed with SOPHIE, CORALIE<sup>8</sup> and HARPS to confirm the planetary nature of the transiting companion and derive the mass of the planet. Figure 3.3 shows CoRoT-2's light curve, and table 3.2 lists the parameters derived for CoRoT-2b and its host star.

The IRF was run with the default values and the IRF-filtered transit signals were fitted, as described in Section 3.2.1. The resulting IRF-filtered light curves along with their transit fit are shown in Fig. 3.4, and the best fit planet parameters in Table 3.2.

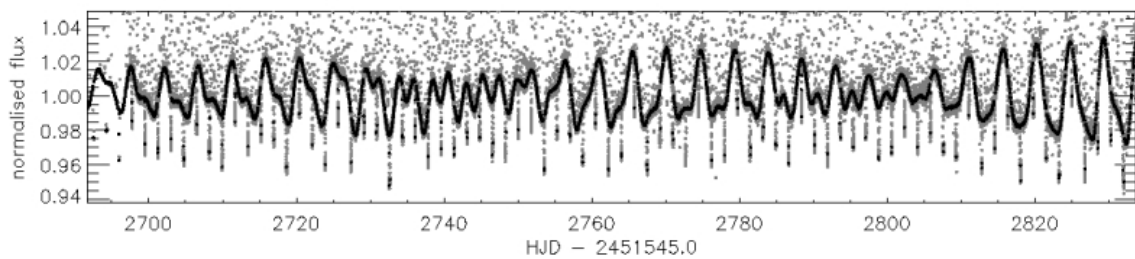


Figure 3.3: CoRoT-2's light curve. Same legend as Figure 3.1.

<sup>8</sup>CORALIE: 50000-resolution echelle spectrograph on the Euler 1.2m telescope at ESO La Silla Observatory, Chile

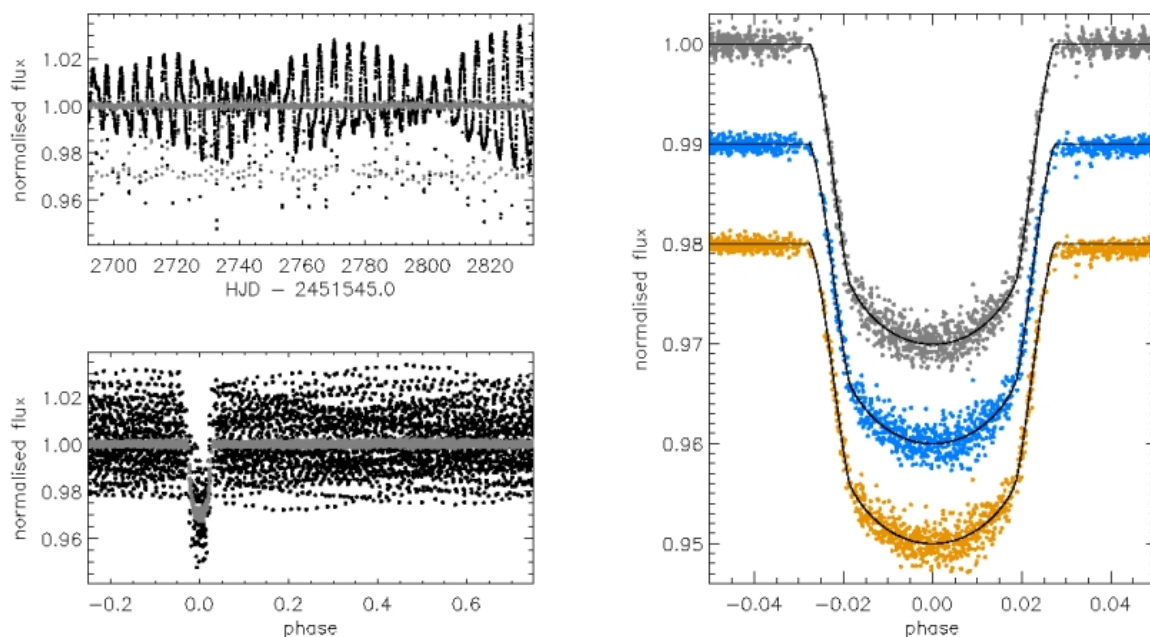


Figure 3.4: The IRF-filtered transit light curve of CoRoT-2b. Same legend as Figure 3.2

Table 3.2: Host star and planet parameters of CoRoT-2b.

Star	Alonso et al. (2008)	this study		
		IRF 0.5d	IRF 0.25d	IRF 0.1d
RA (J2000)	19 <sup>h</sup> 27 <sup>m</sup> 06.5 <sup>s</sup>			
Dec (J2000)	01° 23' 01.5''			
$V_{\text{mag}}$	12.57			
$T_{\text{eff}}$ (K)	5625 ± 120			
$M_{\star}$ ( $M_{\odot}$ )	0.97 ± 0.06			
$R_{\star}$ ( $R_{\odot}$ )	0.902 ± 0.018			
<b>From light curve</b>				
$P$ (d)	1.7429964 ± 0.0000017	same (fixed)	same (fixed)	same (fixed)
$T_0 - 2454237$ (d)	0.53562 ± 0.00014	0.53535 ± 0.00003	0.53541 ± 0.00002	0.53547 ± 0.00002
$R_p/R_{\star}$	0.1667 ± 0.0006	0.1663 ± 0.0008	0.1663 ± 0.0007	0.1662 ± 0.0007
$a/R_{\star}$	6.70 ± 0.03	6.42 ± 0.04	6.38 ± 0.03	6.37 ± 0.03
$i$ (°)	87.8 ± 0.1	86.8 ± 0.2	86.6 ± 0.2	86.6 ± 0.1
$u_a$	0.41 ± 0.03	0.47 ± 0.03	0.45 ± 0.02	0.43 ± 0.02
$u_b$	0.06 ± 0.03	0.03 ± 0.08	0.07 ± 0.06	0.11 ± 0.06
$e$	0 (fixed)	same (fixed)	same (fixed)	same (fixed)
$\frac{M_{\star}^{1/3}}{R_{\star}}$ ( $M_{\odot}, R_{\odot}$ )	1.099 ± 0.005			
$b$	0.26 ± 0.01	0.36 ± 0.02	0.37 ± 0.04	0.38 ± 0.02
<b>Planet</b>				
$M_p$ ( $M_{\text{Jup}}$ )	3.31 ± 0.16			
$R_p$ ( $R_{\text{Jup}}$ )	1.465 ± 0.029			

### 3.2.4 CoRoT-3b

CoRoT-3b is a low mass brown dwarf (BD) with a Jupiter radius and 21 Jupiter masses, orbiting its host star in 4.2 days. This planet was observed with CoRoT nearly continuously for 112 days from May 26th 2007. The discovery of this planet was published in Deleuil et al. (2008). Radial velocity measurements of the star were performed with SOPHIE, TLS<sup>9</sup>, CORALIE, HARPS, and SANDIFORD<sup>10</sup> to confirm the nature of the transiting companion and derive its mass. The parameters of CoRoT-3b are refined in (Triaud et al., 2009). Table 3.3 lists the parameters derived for CoRoT-3b and its host star.

Before running the IRF, the points affected by sudden jumps in flux before 2698 days, from 2737 to 2741 days and from 2745 to 2748 days (in HJD-2451545), were cut out. The IRF was run with the default values as described in Section 3.2.1. Before fitting the transit, for each of the IRF-filtered versions of CoRoT-3's light curve, a correction from the local slope about the phase-folded transit needed to be applied. A 2<sup>nd</sup> order polynomial function was fitted about the phase-folded IRF-filtered light curve and divided into the phase-folded transit. The IRF-filtered transit signals, with their local polynomial fit removed, were then fitted as described in Section 3.2.1. The resulting IRF-filtered light curves along with their transit fit are shown in Fig. 3.6, and the best fit planet parameters in Table 3.3.

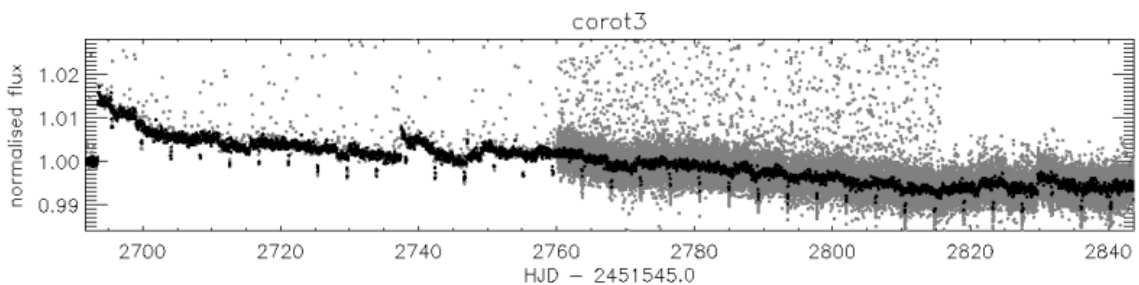


Figure 3.5: CoRoT-3's light curve. Same legend as Figure 3.1.

<sup>9</sup>30000-resolution echelle spectrograph on the 2-m Alfred Jensch telescope in Tautenburg, Germany  
<sup>10</sup>60000-resolution echelle spectrograph on the 2.1m Otto Struve telescope at the McDonald Observatory, Texas, USA

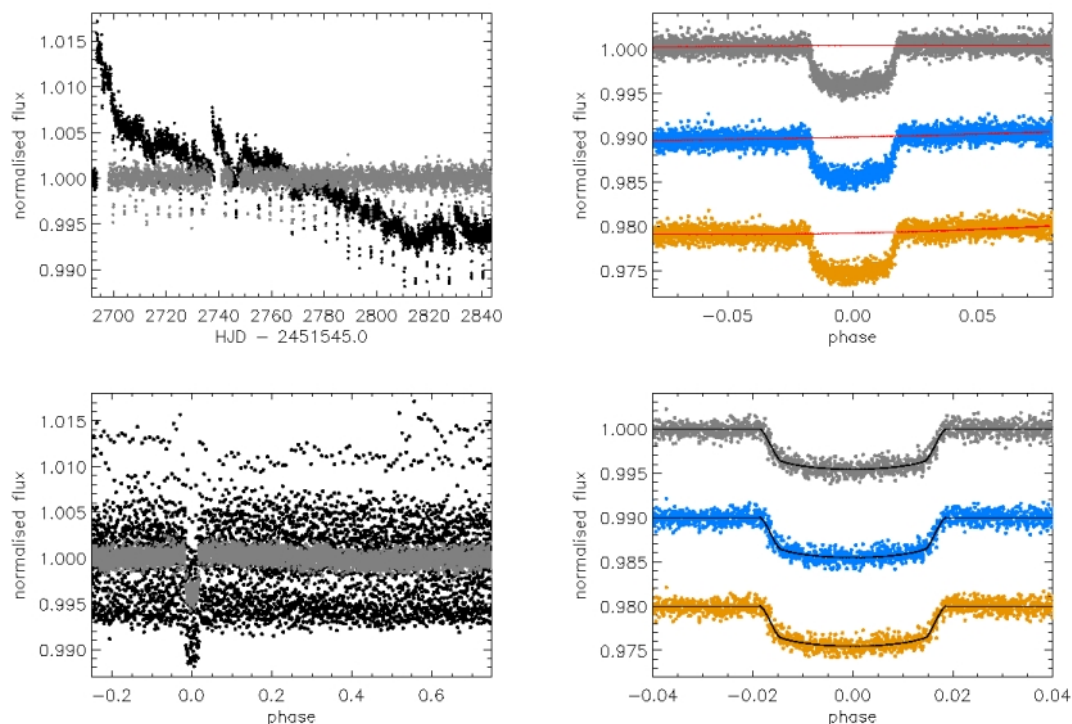


Figure 3.6: The IRF-filtered transit light curve of CoRoT-3b. Same legend as Figure 3.2. The red lines (top right panel) are the  $2^{nd}$  order polynomial fits about the phase-folded IRF-filtered transits that were used to produce the corrected phase-folded transits (bottom right panel) which were then fitted to derive the planet parameters.

Table 3.3: Host star and planet parameters of CoRoT-3b.

	Triaud et al. (2009) & Deleuil et al. (2008)	IRF 0.5d	this study IRF 0.25d	IRF 0.1d
<b>Star</b>				
RA (J2000)	19 <sup>h</sup> 28 <sup>m</sup> 13.26 <sup>s</sup>			
Dec (J2000)	00° 07' 18.7 <sup>''</sup>			
$M_*$ ( $M_\odot$ )	1.37 <sup>+0.059</sup> <sub>-0.043</sub>			
$R_*$ ( $R_\odot$ )	1.540 <sup>+0.083</sup> <sub>-0.078</sub>			
$T_{\text{eff}}$ (K)	6740 ± 140			
log $g$	4.22 ± 0.07			
[Fe/H]	-0.02 ± 0.06			
<b>From light curve</b>				
$P$ (d)	4.2567994 <sup>+0.0000039</sup> <sub>-0.0000031</sub>	same (fixed)	same (fixed)	same (fixed)
$T_0$ -2454283 (d)	0.13388 <sup>+0.00026</sup> <sub>-0.00022</sub>	0.13945 ± 0.00022	0.13947 ± 0.00022	0.13937 ± 0.00022
$R_p/R_*$	0.06632 <sup>+0.00063</sup> <sub>-0.00069</sub>	0.0680 ± 0.0014	0.0676 ± 0.0014	0.0678 ± 0.0015
$a/R_*$	7.96 <sup>+0.43</sup> <sub>-0.35</sub>	7.36 ± 0.41	7.39 ± 0.47	7.38 ± 0.52
$i$ (°)	86.1 <sup>+0.7</sup> <sub>-0.5</sub>	85.1 ± 0.8	85.1 ± 1.0	85.1 ± 1.2
$u_a$	0.23 ± 0.09	0.20 ± 0.27	0.23 ± 0.25	0.25 ± 0.24
$u_b$	0.33 ± 0.09	0.38 ± 0.39	0.34 ± 0.39	0.31 ± 0.38
$\frac{M_*^{1/3}}{R_*}$ ( $M_\odot, R_\odot$ )	0.71 ± 0.04			
$b$	0.54 <sup>+0.13</sup> <sub>-0.09</sub>	0.63 ± 0.15	0.63 ± 0.17	0.63 ± 0.20
<b>From radial velocities</b>				
$e$	0.008 <sup>+0.005</sup> <sub>-0.015</sub>	0 (fixed)	0 (fixed)	0 (fixed)
$\omega$ (°)	179 ± 170	0 (fixed)	0 (fixed)	0 (fixed)
<b>Planet</b>				
$M_p$ ( $M_{\text{Jup}}$ )	21.23 <sup>+0.82</sup> <sub>-0.59</sub>			
$R_p$ ( $R_{\text{Jup}}$ )	0.9934 <sup>+0.058</sup> <sub>-0.058</sub>			

### 3.2.5 CoRoT-4b

CoRoT-4b is a gas-giant planet orbiting its host star in 9.2 days. This planet was observed with CoRoT nearly continuously for 58 days from February 6th 2007. The discovery of this planet was published in Aigrain et al. (2008). Radial velocity measurements of the star was performed with SOPHIE and HARPS to confirm the planetary nature of the transiting companion and derive the mass of the planet. Table 3.4 lists the parameters derived for CoRoT-4b and its host star.

Before running the IRF, the points affected by sudden jumps in flux before 2595 days (in HJD-2451545) were cut out. The IRF was run with the default values as described in Section 3.2.1. Before fitting the transit, for each of the IRF-filtered versions of CoRoT-3's light curve, a correction from the local slope about the phase-folded transit needed to be applied. A  $2^{nd}$  order polynomial function was fitted about  $(-0.008, 0.008)$  phase range) the phase-folded IRF-filtered light curve and divided from the phase-folded transit. The IRF-filtered transit signals, with their local polynomial fit removed, were then fitted as described in Section 3.2.1. The resulting IRF-filtered light curves along with their transit fit are shown in Fig. 3.8, and the best fit planet parameters in Table 3.4.

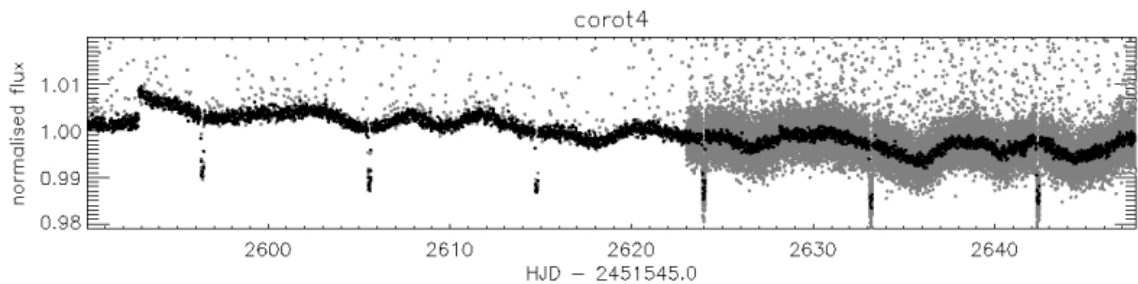


Figure 3.7: CoRoT-4's light curve. Same legend as Figure 3.1.

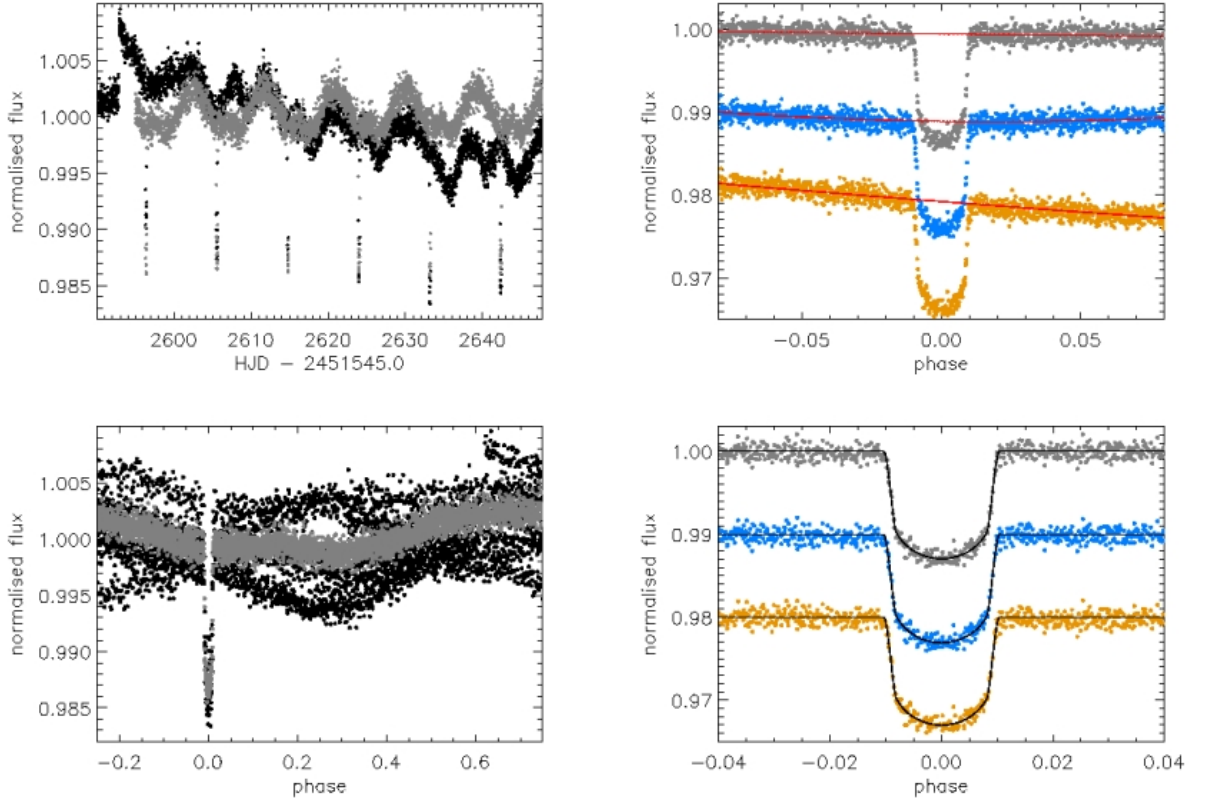


Figure 3.8: The IRF-filtered transit light curve of CoRoT-4b. Same legend as Figure 3.6

Table 3.4: Host star and planet parameters of CoRoT-4b.

	Aigrain et al. (2008) & Moutou et al. (2008)		IRF 0.5d	this study IRF 0.25d	IRF 0.1d
<b>Star</b>					
RA (J2000)	06 <sup>h</sup> 48 <sup>m</sup> 46.70 <sup>s</sup>				
Dec (J2000)	-00° 40' 21.97''				
$R_{\text{mag}}$	13.45				
$P_{\text{rot}}$ (d)	$8.87 \pm 1.12$				
$M_*$ ( $M_{\odot}$ )	$1.16^{+0.03}_{-0.02}$				
$R_*$ ( $R_{\odot}$ )	$1.17^{+0.01}_{-0.03}$				
$v \sin i$ ( $\text{km s}^{-1}$ )	$6.4 \pm 1.0$				
$T_{\text{eff}}$ (K)	$6190 \pm 60$				
$\log g$	$4.41 \pm 0.05$				
<b>From light curve</b>					
$P$ (d)	$9.20205 \pm 0.00037$	Bayesian range	same (fixed)	same (fixed)	same (fixed)
$T_0 - 2454141$ (d)	$0.36416 \pm 0.00089$		$0.36434 \pm 0.00022$	$0.36440 \pm 0.00021$	$0.36439 \pm 0.00020$
$R_p/R_*$	$0.1047^{+0.0041}_{-0.0022}$	0.1000 – 0.1125	$0.1056 \pm 0.0011$	$0.1064 \pm 0.0012$	$0.1054 \pm 0.0011$
$a/R_*$	$17.36^{+0.05}_{-0.25}$	14.30 – 17.80	$16.84 \pm 0.35$	$16.66 \pm 0.39$	$16.82 \pm 0.34$
$i$ (°)	$90.000^{+0.000}_{-0.085}$	87.708 – 90.000	$89.2 \pm 0.4$	$89.1 \pm 0.4$	$89.3 \pm 0.4$
$u_a$	$0.44^{+0.16}_{-0.15}$	0.00 – 1.00	$0.48 \pm 0.08$	$0.50 \pm 0.09$	$0.45 \pm 0.08$
$u_b$	–		$-0.04 \pm 0.17$	$-0.06 \pm 0.18$	$0.05 \pm 0.18$
$\frac{M_*^{1/3}}{R_*} (M_{\odot}, R_{\odot})$	$0.899^{+0.003}_{-0.013}$	0.741 – 0.922	0 (fixed)	0 (fixed)	0 (fixed)
$e$	$0.0 \pm 0.1$		0 (fixed)	0 (fixed)	0 (fixed)
$b$	$0.0^{+0.03}_{-0.0}$	0 – 0.57	$0.22 \pm 0.14$	$0.26 \pm 0.14$	$0.20 \pm 0.13$
<b>Planet</b>					
$M_p (M_{\text{Jup}})$	$0.72 \pm 0.08$				
$R_p (R_{\text{Jup}})$	$1.19^{+0.06}_{-0.05}$				



### 3.2.6 CoRoT-5b

CoRoT-5b is a Jupiter-size planet orbiting its host star in 4 days. This planet was observed with CoRoT nearly continuously for 112 days from October 24th 2007. The discovery of this planet was published in Rauer et al. (2009). Radial velocity measurements of the host star were performed with SOPHIE and HARPS to confirm the planetary nature of the transiting companion and derive the mass of the planet. Table 3.5 lists the parameters derived for CoRoT-5b and its host star.

Before running the IRF, the points affected by sudden jumps in flux before 2858 days, (time as displayed in Fig 3.9), were cut out. The IRF was run with the default values as described in Section 3.2.1. Before fitting the transit, for each of the IRF-filtered versions of CoRoT-3's light curve, a correction from the local slope about the phase-folded transit needed to be applied. A  $2^{nd}$  order polynomial function was fitted about  $(-0.008, 0.008)$  phase range) the phase-folded IRF-filtered light curve and divided from the phase-folded transit. The IRF-filtered transit signals, with their local polynomial fit removed, were then fitted as described in Section 3.2.1. The resulting IRF-filtered light curves along with their transit fit are shown in Fig. 3.10, and the best fit planet parameters in Table 3.5.

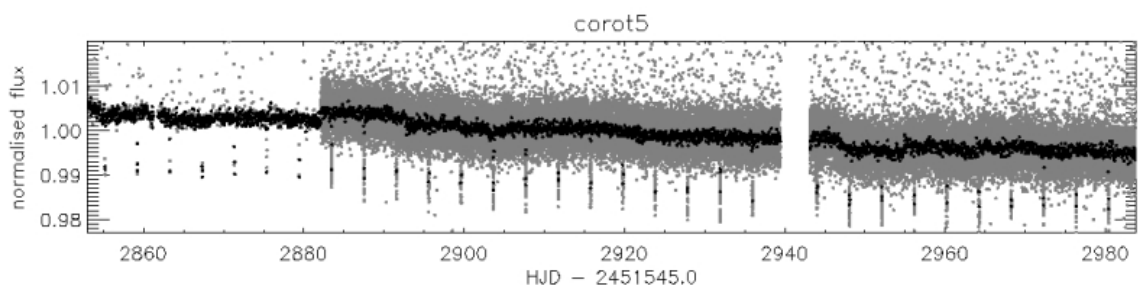


Figure 3.9: CoRoT-5's light curve. Same legend as Figure 3.1.

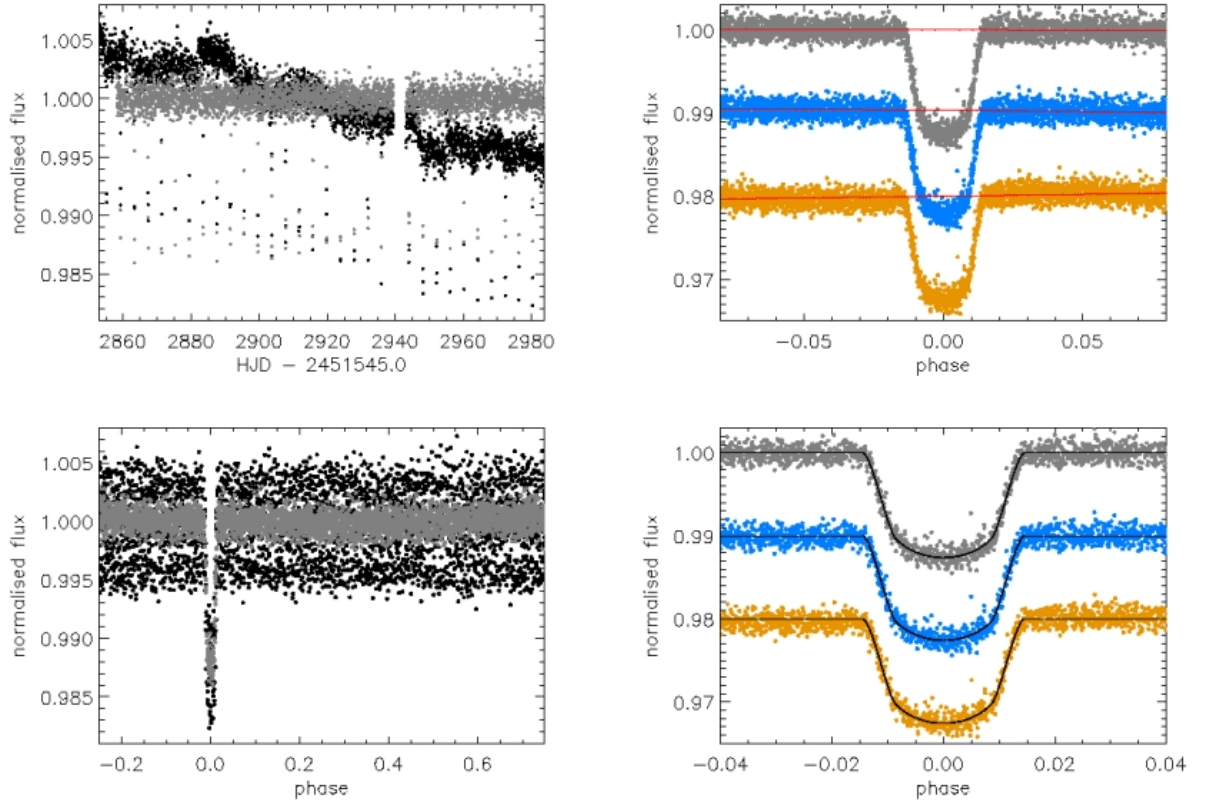


Figure 3.10: The IRF-filtered transit light curve of CoRoT-5b. Same legend as Figure 3.6

Table 3.5: Host star and planet parameters of CoRoT-5b.

	Rauer et al. (2009)	IRF 0.5d	this study IRF 0.25d	IRF 0.1d
<b>Star</b>				
RA (J2000)	06 <sup>h</sup> 45 <sup>m</sup> 07 <sup>s</sup>			
Dec (J2000)	00° 48' 55"			
$V_{\text{mag}}$	14.0			
$M_*$ ( $M_{\odot}$ )	$1.00 \pm 0.02$			
$R_*$ ( $R_{\odot}$ )	$1.186 \pm 0.04$			
$T_{\text{eff}}$ (K)	$6100 \pm 65$			
$\log g$	$4.189 \pm 0.03$			
[Fe/H]	$-0.25 \pm 0.06$			
<b>From light curve</b>				
$P$ (d)	$4.0378962 \pm 0.0000019$	same (fixed)	same (fixed)	same (fixed)
$T_0 - 2454400$ (d)	$0.19885 \pm 0.0002$	$0.19843 \pm 0.00015$	$0.19846 \pm 0.00015$	$0.19799 \pm 0.00018$
$R_p/R_*$	$0.12087^{+0.00021}_{-0.00023}$	$0.1135 \pm 0.0021$	$0.1139 \pm 0.0024$	$0.1135 \pm 0.0022$
$a/R_*$	$8.97 \pm 0.31$	$9.39 \pm 0.20$	$9.40 \pm 0.20$	$9.39 \pm 0.24$
$i$ (°)	$85.83^{+0.99}_{-1.38}$	$85.7 \pm 0.2$	$85.7 \pm 0.2$	$85.7 \pm 0.2$
$u_a$	0.308 fixed	$0.13 \pm 0.33$	$0.24 \pm 0.36$	$0.19 \pm 0.34$
$u_b$	0.308 fixed	$0.69 \pm 0.45$	$0.54 \pm 0.50$	$0.62 \pm 0.48$
$\frac{M_p^{1/3}}{R_*} (M_{\odot}, R_{\odot})$	$0.843 \pm 0.024$			
$b$	$0.90^{+0.25}_{-0.17}$	$0.71 \pm 0.05$	$0.71 \pm 0.05$	$0.71 \pm 0.06$
<b>From radial velocities</b>				
$e$	$0.09^{+0.09}_{-0.04}$	0 (fixed)	0 (fixed)	0 (fixed)
$\omega$ (°)	$-128^{+289}_{-48}$	0 (fixed)	0 (fixed)	0 (fixed)
<b>Planet</b>				
$M_p (M_{\text{Jup}})$	$0.467^{+0.047}_{-0.024}$			
$R_p (R_{\text{Jup}})$	$1.388^{+0.046}_{-0.047}$			

### 3.2.7 CoRoT-6b

CoRoT-6b is a Jupiter-size planet orbiting its host star in 8.9 days. This planet was observed with CoRoT nearly continuously for 144 days from April 15th 2008. The discovery of this planet was published in Fridlund et al. (2010). Radial velocity measurements of the host star were performed with SOPHIE to confirm the planetary nature of the transiting companion and derive the mass of the planet. Table 3.6 lists the parameters derived for CoRoT-6b and its host star.

Before running the IRF, the points affected by sudden jumps in flux before 3031 days, and from 3152 to 3153.54 days (time as displayed in Fig 3.9), were cut out. The IRF was run with the default values as described in Section 3.2.1. Before fitting the transit, for each of the IRF-filtered versions of CoRoT-6's light curve, a correction from the local slope about the phase-folded transit needed to be applied. A  $2^{nd}$  order polynomial function was fitted about the phase-folded IRF-filtered light curve and divided into the phase-folded transit. The IRF-filtered transit signals, with their local polynomial fit removed, were then fitted as described in Section 3.2.1. The resulting IRF-filtered light curves along with their transit fit are shown in Fig. 3.12, and the best fit planet parameters in Table 3.6.

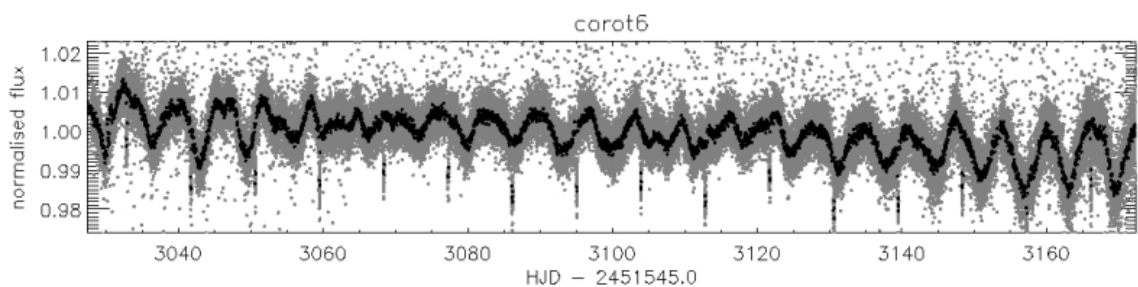


Figure 3.11: CoRoT-6's light curve. Same legend as Figure 3.1.

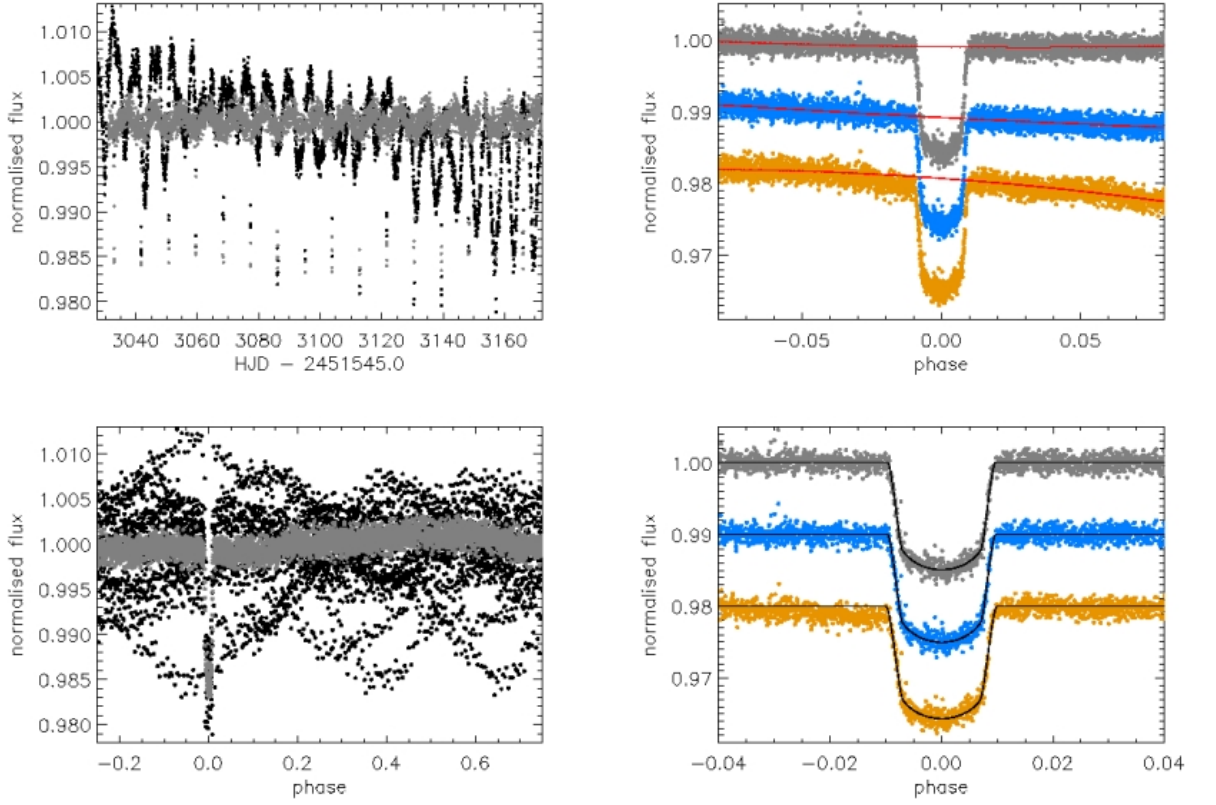


Figure 3.12: The IRF-filtered transit light curve of CoRoT-6b. Same legend as Figure 3.6

Table 3.6: Host star and planet parameters of CoRoT-6b.

	Fridlund et al. (2010)	IRF 0.5d	this study IRF 0.25d	IRF 0.1d
<b>Star</b>				
RA (J2000)	18 <sup>h</sup> 44 <sup>m</sup> 17.42 <sup>s</sup>			
Dec (J2000)	06° 39' 47.95''			
$V_{\text{mag}}$	13.9			
$M_*$ ( $M_\odot$ )	$1.055 \pm 0.055$			
$R_*$ ( $R_\odot$ )	$1.025 \pm 0.026$			
$T_{\text{eff}}$ (K)	$6090 \pm 70$			
$\log g$	$4.3 \pm 0.1$			
[Fe/H]	$-0.2 \pm 0.1$			
<b>From light curve</b>				
$P$ (d)	$8.886593 \pm 0.000004$	same (fixed)	same (fixed)	same (fixed)
$T_0-2454595$ (d)	$0.6144 \pm 0.0002$	$0.61434 \pm 0.00013$	$0.61424 \pm 0.00013$	$0.61323 \pm 0.00040$
$R_p/R_*$	$0.11687 \pm 0.00092$	$0.1147 \pm 0.0015$	$0.1150 \pm 0.0014$	$0.1185 \pm 0.0050$
$a/R_*$	$17.9 \pm 0.3$	$17.62 \pm 0.42$	$17.51 \pm 0.42$	$16.39 \pm 1.16$
$i$ (°)	$89.1 \pm 0.3$	$88.9 \pm 0.3$	$88.9 \pm 0.3$	$88.4 \pm 0.5$
$u_a$	$0.35 \pm 0.14$	$0.18 \pm 0.10$	$0.17 \pm 0.10$	$0.06 \pm 0.16$
$u_b$	$0.23 \pm 0.14$	$0.52 \pm 0.21$	$0.54 \pm 0.21$	$0.69 \pm 0.35$
$\frac{M_*^{1/3}}{R_*}$ ( $M_\odot, R_\odot$ )	$0.993 \pm 0.018$			
$b$	0.28 (0 - 0.56)	$0.32 \pm 0.10$	$0.34 \pm 0.10$	$0.45 \pm 0.20$
<b>From radial velocities</b>				
$e$	< 0.1	0 (fixed)	0 (fixed)	0 (fixed)
<b>Planet</b>				
$M_p$ ( $M_{\text{Jup}}$ )	$2.96 \pm 0.34$			
$R_p$ ( $R_{\text{Jup}}$ )	$1.166 \pm 0.035$			

### 3.2.8 CoRoT-7b

CoRoT-7b is a Super-Earth planet orbiting its host star in 0.85 days. The discovery of this planet was published in Léger et al. (2009). Due to the small size of the planet and the activity level of its host stars, confirming this planet with its mass derived from radial velocity measurement was a very challenging task. The planetary nature of this planet was thus first claimed with an upper limit on its mass  $< 21M_{\oplus}$  (based on radial velocity measurements with SOPHIE) and intensive ground-based follow-up (photometry, imaging, spectroscopy) to exclude probability of the transits been stellar eclipses. Later, HARPS radial velocity follow-up (Queloz et al., 2009) revealed CoRoT-7 as a multiple planetary system. Table 3.7 lists the parameters derived for CoRoT-7b and its host star.

The IRF was run as described in Section 3.2.1 but with a bin size of 0.0024 in phase (IRF `binsize` parameter) and a convergence limit of  $1. \cdot 10^{-8}$  (IRF `cvlim` parameter). The three smoothing timescales to estimate the stellar variability were also tested (IRF `timescale` parameter): 0.50, 0.25 and 0.10 days. The IRF-filtered transit signals were then fitted as described in Section 3.2.1. For the fits, because of the low signal-to-noise ratio of the transit, the values of the quadratic limb darkening parameters were fixed to the values in CoRoT-7b discovery paper (Léger et al., 2009) – and not adjusted as done for the other planets. The resulting IRF-filtered light curves along with their transit fit are shown in Fig. 3.14, and the best fit planet parameters in Table 3.7.

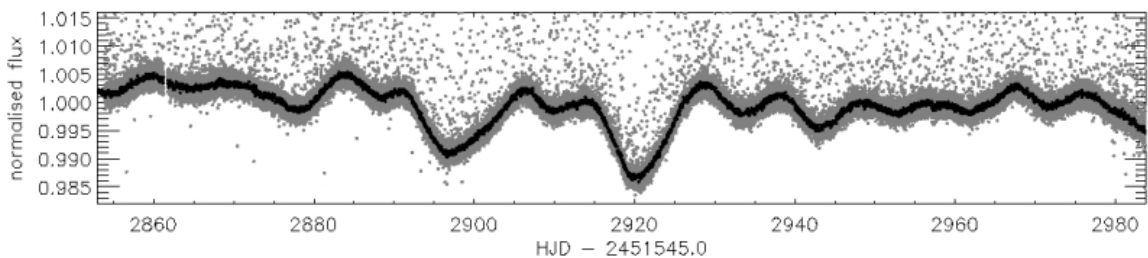


Figure 3.13: CoRoT-7's light curve. Same legend as Figure 3.1.

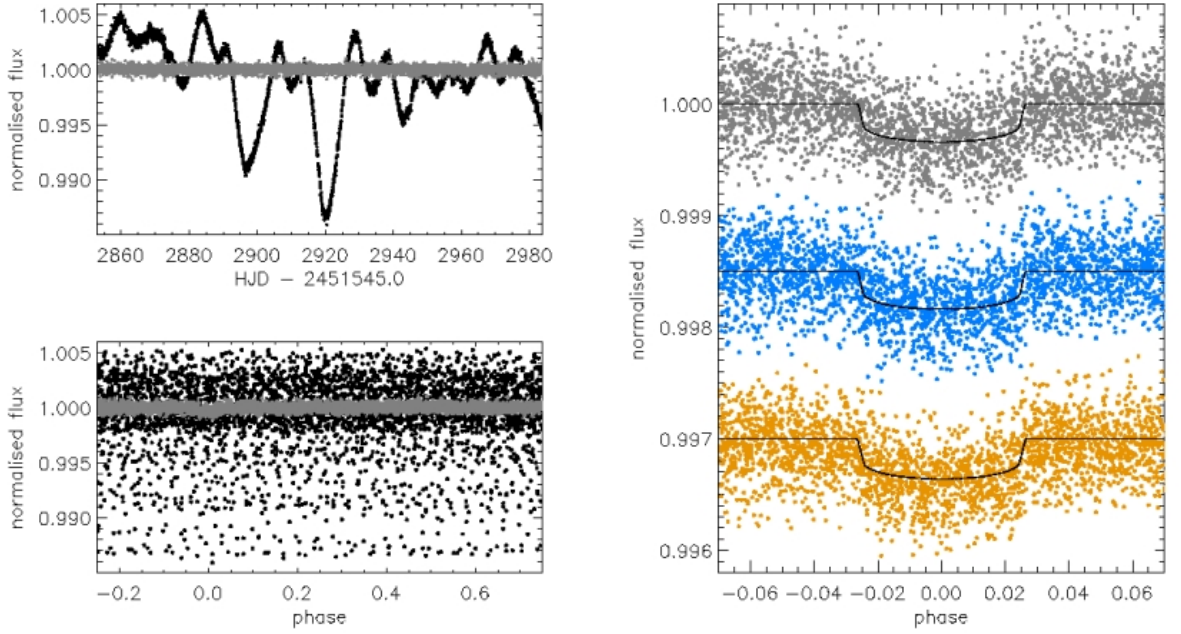


Figure 3.14: The IRF-filtered transit light curve of CoRoT-7b. Same legend as Figure 3.2

Table 3.7: Host star and planet parameters of CoRoT-7b.

	Léger et al. (2009) & Queloz et al. (2009)	IRF 0.5d	this study IRF 0.25d	IRF 0.1d
<b>Star</b>				
RA (J2000)	06 <sup>h</sup> 43 <sup>m</sup> 49.0 <sup>s</sup>			
Dec (J2000)	-01° 03' 46.0''			
$V_{\text{mag}}$	11.668 ± 0.008			
$T_{\text{eff}}$ (K)	5275 ± 75			
log $g$	4.50 ± 0.10			
[Fe/H]	+0.03 ± 0.06			
Spectral Type	G9 V			
$M_*$ ( $M_{\odot}$ )	0.93 ± 0.03			
$R_*$ ( $R_{\odot}$ )	0.87 ± 0.04			
<b>From light curve</b>				
$P$ (d)	0.853585 ± 0.000024	same (fixed)	same (fixed)	same (fixed)
$T_0$ -2454398 (d)	0.0767 ± 0.0015	0.07726 ± 0.00037	0.07716 ± 0.00031	0.07682 ± 0.00030
$R_p/R_*$	0.0187 ± 0.0003	0.0184 ± 0.0013	0.0182 ± 0.0012	0.0186 ± 0.0015
$a/R_*$	4.27 ± 0.20	4.13 ± 1.4	4.31 ± 1.2	4.70 ± 1.3
$i$ (°)	80.1 ± 0.3	79.3 ± 11.1	80.1 ± 8.8	81.9 ± 12.6
$u_a$	0.40	same (fixed)	same (fixed)	same (fixed)
$u_b$	0.20	same (fixed)	same (fixed)	same (fixed)
$b$	0.73 ± 0.06	0.77 (0 - 1)	0.74 (0 - 1)	0.66 (0 - 1)
<b>From radial velocities</b>				
$e$	0	0 (fixed)	0 (fixed)	0 (fixed)
<b>Planet</b>				
$M_p$ ( $M_{\oplus}$ )	4.8 ± 0.8			
$R_p$ ( $R_{\oplus}$ )	1.68 ± 0.09			

### 3.2.9 Discussion

For all the objects studied in this chapter, except CoRoT-6b, the parameters derived from the IRF-filtered light curves with different timescale are consistent with each other within  $1\sigma$  ( $\sigma$  being the uncertainty on the parameter). This shows that IRF-filtering down to timescale=0.25 days still preserves the transit shape within the noise limit, but smaller timescale values affect the transit shape in some cases.

Compare to the planet/brown dwarf parameters published in the discovery of the first seven CoRoT planets/brown dwarfs, the adjusted planet parameters and quadratic limb darkening coefficients, derived from the fitting of the IRF-filtered transit light curve using a Levenberg-Marquardt algorithm, are consistent within  $1\sigma$  for CoRoT-2b, CoRoT-4b, CoRoT-6b and CoRoT-7b, consistent within  $2\sigma$  for CoRoT-3b, and different (outside the  $2\sigma$  range) for CoRoT-1b and CoRoT-5b.

The difference in the limb darkening coefficients is expected to contribute to the difference in the planet parameters, in particular for  $R_p/R_*$ . This can explain the cases where the parameters derived in this chapter are different by more than  $2\sigma$  from the parameters published in the discovery paper of the respective planets.

The errors bars derived in the chapter are smaller for CoRoT-1b and CoRoT-4b, larger for CoRoT-7b, and similar for the other planets and the brown dwarf. Fitting the limb darkening on a light curve with not enough photometric precision increases the error bars on all the other parameters. The alternative approach is to fix the limb darkening coefficients to the value derived from stellar atmosphere models for the stellar atmospheric parameters of the host star ( $T_{\text{eff}}$ ,  $\log g$ , (M/H)), in the observed filter (here, the CoRoT bandpass), and a chosen limb darkening law. Claret (2000) and Claret (2004) give tables of limb darkening coefficients for different standard filters and Sing (2010) for CoRoT and Kepler bandpasses. The larger uncertainties found for the planet parameters of CoRoT-7b are more representative of the noise level in the light curve than the values publishes in the planet discovery paper. For CoRoT-1b and CoRoT-2b, the smaller uncertainties derived for the planet parameters can come from a reduction in the noise of the filtered transit light curve achieved with the IRF.

In CoRoT-2's light curve, IRF-filtered with timescale = 0.5 days, some high frequency variations can be seen. What causes these features is not well understood. They often appear when binning the phase folded light curve with a section of the light curve shifted (not in phase) from another one, for instance due to an inaccurate transit period or wrong time stamps.

In CoRoT-3,4,5 's light curves, residual stellar variability at the planet orbital period can be seen even after IRF-filtering down to timescale = 0.10 days. Thus, the rotation period of these stars must be close to a multiple of the orbital period of their transiting planet, making the residual stellar variability difficult to separate from the transit signal. The additional variability at the orbital period of the planet could be caused by a planet-star interaction.

In CoRoT-6's light curve, IRF-filtered with  $\text{timescale} = 0.10$  days, there is a drop in flux ( $\sim 5\%$  of the transit depth lasting for  $\sim 0.015$  phase units) just before the transit. This feature affects the evaluation of the transit shape and thus the derived planet parameters, which can be seen in the larger difference in the planet parameters derived. This feature is likely to have been created by the IRF (see explanations in Chapter 4, Section 4.2.4).

### 3.3 IRF performance on CoRoT space data

For all the planets, the IRF allows filtering of stellar variability to lower time scales (down to 6 h) without affecting the shape of the phase folded transit. This is a significant improvement from standard filters that would have affected the transit signal with this level of filtering.

For all the planets, the difference between the planet parameter values in the literature and those derived with the IRF-filtered light curves ( $\text{timescale} 0.50$  and  $0.25$  days) is within the error bar associated to each parameter. This shows, on one hand, that the IRF is performing well as it is not affecting the transit shape, and on the other hand, that the traditional variability filtering method, such as those used in the discovery papers, are appropriate for the levels of stellar variability in those light curves. The improvement in the planet parameters after IRF-filtering was more obvious in the CoRoT BT2 simulated data used in Chapter 2. This reflects the lower level of stellar activity (lower amplitude, longer timescales) of stars with planets discovered by CoRoT, compared to the activity level modelled in the simulated data. The apparent lower activity level of stars with planet could also be a detection bias, as planets around active stars are more difficult to detect.

#### 3.3.1 Limitations

The IRF is a post-detection method, it requires a prior knowledge of the period of the signal to be reconstructed, it cannot be used without a good estimate of this period.

The IRF reconstructs the signal in its phase folded shape, and therefore its direct product is an average over all the individual transits and has lost the information on transit shape variation with time due to perturbation by another planet for instance. Another approach would need to be taken to study such time-variations.

#### 3.3.2 Future work

Adjusting the limb darkening coefficients simultaneously has an influence on the value of  $R_p/R_*$  derived from the transit. It will be interesting to see how the parameters compare with the values in the planet discovery papers, for the same model of the limb



darkening. This will allow to check the difference in transit depth free from the limb darkening-transit depth degeneracy.

It will be interesting to look for time-variations of the transit shape in the residuals of the light curve with the transit fit to the phase-folded IRF-filtered light curve removed. Time-variations in the transit shape can be due for instance to features on the stellar surface or to another planet perturbing the orbit of the transiting planet.

As the IRF reconstructs all signal at the orbital period of the planet, one can attempt a search for other planet orbital feature in the IRF-filtered light curve, such as the planet secondary eclipse and the planet orbital phase variations. This aspect is studied in Chapter 4.